Granular Matter
DOI 10.1007/s10035-007-0056-0

Casimir forces in granular and other non equilibrium systems

R. Brito · R. Soto · U. Marini Bettolo Marconi

Received: 6 April 2007

Abstract In this paper we present a method to calculate Casimir Forces for non equilibrium systems with long range correlations. The origin of the force are the fluctuating fields, and the modification that the external, macroscopic objects induce in the spectrum of the fluctuations. The method is first illustrated with a simple model: a reaction-diffusion non-equilibrium system with an structure factor that possesses a characteristic length. The second part of the paper deals with a granular fluid where correlations are long ranged at all scales. In the first case the hydrodynamic fluctuations are confined by two plates, while in the second one the confinement comes from two immobile large and heavy particles. In both cases Casimir forces are calculated, and their properties analyzed.

Keywords Non-equilibrium systems · Long range correlations · Casimir forces · Granular matter

1 Introduction

There are forces in Physics that do not derive from a potential energy: Coriolis force, centrifugal force, static and dynamic frictional forces, just to mention a few. Casimir forces belong to this class. They were discovered by Casimir in 1948 [1], by applying Heisenberg's uncertainty principle to the vacuum fluctuations of the Electromagnetic field. Casimir found that two flat metallic parallel plates attract with a force per unit area given by $F/A = -\hbar c \pi^2/(240x^4)$. This force has been measured with high precision by Lamoreau [2,3] and Mohideen and coworkers [4,5]. For a recent review see [6].

More recently, Casimir forces of non-quantal origin, have been considered (see, e.g. the review [7]). In this case, the forces do not result from Heisenberg's principle, but are, for instance, originated from thermal fluctuations, so that their amplitude is proportional to $k_B T$, the absolute temperature times the Boltzmann constant, and not to the Planck constant times the speed of light $\hbar c$. The fluctuating field, instead of being the Electromagnetic radiation, can be an hydrodynamic field such as density, temperature, concentration, director vector, etc. When the fluctuating system is confined between two plates, the fluctuation spectrum is modified by the associated boundary conditions. As a result both the (free) energy density and the stress tensor become size dependent. Therefore, the stress tensor in the region between the two plates and outside them are different, leading to the appearance of Casimir forces. The unifying feature is the presence of long spacial correlations $G(r)$ which make that the confined system is effectively affected by the imposed boundary conditions, therefore modifying the value of the (free) energy density and the stress tensor. The long range correlations manifest in static structure factors $S(\mathbf{k})$, Fourier Transforms of $G(r)$, that decay in algebraic manner, with some inverse power of the wave vector $\mathbf{k}$. Such long range correlations may appear in near critical *Equilibrium systems* (e.g. in fluids in the vicinity of a critical point [8–11]), or from a broken continuum symmetry [12] (like liquid crystals in smectic or nematic phases [13,14]) superfluid films

R. Brito (✉)
Dept. de Física Aplicada I and GISC, Universidad Complutense, 28040 Madrid, Spain
e-mail: brito@fis.ucm.es

R. Soto
Departamento de Física, FCFM, Universidad de Chile, Casilla 487-3, Santiago, Chile
e-mail: rsoto@dfi.uchile.es

U. Marini Bettolo Marconi
Dipartimento di Fisica, Università di Camerino, 62032 Camerino, Italy
e-mail: Umberto.Marini.Bettolo@roma1.infn.it

[15] colloidal systems [16], etc. For most of these systems Casimir forces have been derived. The approach to compute the force is the same as originally proposed by Casimir, that is compute the size dependent free energy and differentiate it with respect to distance. Also, the size dependent stress tensor can be computed directly using the scale invariance feature of critical fluids [10,17], scale-free non-equilibrium systems [18], and critical spin models [19].

However, there is also a whole class of systems where long range correlations are the norm: *non-equilibrium systems*. We can group them under two items:

(i) Systems under non equilibrium constraints like spatial gradients [20]: fluids under shear, plane Couette flow, [21,22], Rayleigh–Benard cell under a temperature gradient [23–25], or systems under concentration gradients [26], where the structure factor is $S(k) \sim 1/(k^2 + k_0^2)$, being k_0 the inverse of a characteristic length in the system.

(ii) Systems without *detailed balance*. For instance, it has been shown [27–29] that systems described by the Langevin equation with conservative dynamics and non-conservative noise have long range spatial and temporal correlations. Analogously, non-equilibrium concentration fluctuations in reaction diffusion systems can be long ranged under certain conditions [30] and granular systems, where the collisional dissipation and the energy injection break the detailed balance property and hence develop long range correlations [31,32]. These two systems will be described in this paper. Long range correlations caused by absence of detailed balance are present in other non equilibrium systems like kinetic growth models [33,34], traffic flows [35,36], anisotropic diffusion [37], Lattice gases [38,39], inelastic Maxwell molecules [40,41] among others.

2 Casimir forces in nonequilibrium systems

As an example of how a Casimir force arises in a non-equilibrium system with long range correlations, we consider the simple case of a reaction-diffusion system in three dimensions [42], where the fluctuating density n around the homogeneous reference density n_0 obeys the equation

$$\frac{\partial \phi}{\partial t} = \nabla \cdot (D\nabla\phi + \boldsymbol{\xi}_1) - \lambda\phi + \xi_2, \tag{1}$$

where $\phi = n - n_0$ is the fluctuating field, D is the diffusion coefficient, and $\lambda > 0$ is the relaxation rate. The terms $\boldsymbol{\xi}_1$ and ξ_2 describe fluctuations in the diffusive flux and in the reaction rate, corresponding to conservative and non-conservative noises, respectively. They are assumed to have white noise spectrum

$$\begin{aligned} \langle \xi_{1i}(\mathbf{r}, t)\xi_{1k}(\mathbf{r}', t')\rangle &= \Gamma_1 \delta_{i,k}\delta(\mathbf{r}-\mathbf{r}')\delta(t-t'), \\ \langle \xi_2(\mathbf{r}, t)\xi_2(\mathbf{r}', t')\rangle &= \Gamma_2\delta(\mathbf{r}-\mathbf{r}')\delta(t-t'). \end{aligned} \tag{2}$$

The solution of Eq. (1) predicts that, after an initial transient, the density ϕ is statistically homogeneous and stationary so that in Fourier space we have:

$$\langle \phi_{\mathbf{k}}\rangle = 0, \quad \langle \phi_{\mathbf{k}}\phi_{\mathbf{q}}\rangle = V S(\mathbf{k})\delta_{\mathbf{k},-\mathbf{q}}, \tag{3}$$

where the symbol $\langle\cdot\rangle$ represents the average over the two noises $\boldsymbol{\xi}_1$ and ξ_2. The structure factor $S(\mathbf{k})$ is given by (see e.g. Chap. (8.3) of [30]):

$$S(\mathbf{k}) = \frac{\Gamma_1 k^2 + \Gamma_2}{2(Dk^2+\lambda)} = \frac{\Gamma_1}{2D} + \frac{\Gamma/2D}{k^2+k_0^2}, \tag{4}$$

with $\Gamma = \Gamma_2 - \Gamma_1\lambda/D$ and $k_0 = \sqrt{\lambda/D}$. The corresponding real space density–density correlation, which is obtained as the Fourier transform of $S(\mathbf{k})$, reads

$$G(\mathbf{r}) = \frac{\Gamma_1}{2D}\delta(\mathbf{r}) + \frac{\Gamma}{2D}\frac{e^{-k_0 r}}{r}. \tag{5}$$

The second contribution, stemming from the k-dependent term in (4), represents fluctuations with a correlation length that depends on the reaction parameters, λ and D, and therefore, are of macroscopic size. In particular, the system described by Eq. (1) has a critical point at $\lambda = 0$ and near it the correlation length diverges. If the reaction satisfies the fluctuation–dissipation theorem [30,42,43] then $\Gamma_1 = 2k_B T D$ and $\Gamma_2 = 2k_B T\lambda$, where T is the temperature, implying that Γ vanishes along with the macroscopic correlations. On the contrary, in non-equilibrium systems which violate the fluctuation–dissipation theorem, Γ does not vanish and macroscopic correlations are present. The δ-term of $G(\mathbf{r})$ in Eq. (4), coming from $\Gamma_1/2D$, describes the microscopic self-correlation of the particles that a mesoscopic model, valid for larger length scales, cannot resolve. These correlations are present both in equilibrium and non-equilibrium and as it will become manifest in the next paragraphs they do not contribute to the Casimir forces. Therefore, they will be eliminated henceforth. This corresponds to subtracting the asymptotic value of S for large values of k. Hereafter, we will consider the macroscopic part (or, equivalently, the non-equilibrium part) of the structure factor $S^*(\mathbf{k}) = S(\mathbf{k}) - \lim_{k\to\infty} S(k) = \Gamma/[2D(k^2+k_0^2)]$. This is equivalent to suppress the vectorial (conserved) noise $\boldsymbol{\xi}_1$ and keep only a scalar (non-conserved) noise ξ with an intensity Γ.

We study now the effect of confining the system between two plates, parallel and infinite in the y and z-directions, located at $x = 0$ and $x = L$, and calculate if the confinement of the fluctuating field produce a Casimir force between the plates surrounded by a fluid described by Eq. (1). The force derives from the pressure, that we will assume depend on the local density $p(n)$, exerted by the particles over the plates. To proceed, we consider the system in a volume $L_x \times L_y \times L_z$, periodic in all directions. In this volume we place two plates at distance L with non flux boundary conditions at them, as natural for a reacting system. The total volume V results divided into two regions: Region I in between the plates of volume $L \times L_y \times L_z$, and Region II outside the plates of volume $(L_x - L) \times L_y \times L_z$. The limit $L_x, L_y, L_z \to \infty$ will eventually be taken.

In order to perform the analysis in the two regions let us consider a case of a general volume $V = X \times L_y \times L_z$, where $X = L$ for Region I and $X = L_x - L$ for Region II. The density field is expanded, taking into account the non flux boundary conditions on the x-direction, as

$$\phi(\mathbf{r}, t) = V^{-1} \sum_{k_x} \sum_{k_y} \sum_{k_z} \phi_{\mathbf{k}}(t) \cos(k_x x) e^{i k_y y} e^{i k_z z}, \qquad (6)$$

where $k_x = \pi n_x / X$, $k_y = 2\pi n_y / L_y$, $k_z = 2\pi n_z / L_z$, $n_x = 0, 1, 2, \ldots$ and $n_y, n_z = \cdots, -1, 0, 1, \ldots$. The noise ξ is expanded in a similar way with

$$\langle \xi_{\mathbf{k}}(t) \xi_{\mathbf{q}}(t') \rangle = \gamma_{k_x} V \Gamma \hat{\delta}_{\mathbf{k},\mathbf{q}} \delta(t - t'), \qquad (7)$$

where $\hat{\delta}_{\mathbf{k},\mathbf{q}} = \delta_{k_x,q_x} \delta_{k_y,-q_y} \delta_{k_z,-q_z}$ is a modified 3D Kronecker delta. Moreover the factor γ_{k_x} ($\gamma_{k_x} = 1/2$ if $k_x = 0$ and $\gamma_{k_x} = 1$ otherwise) appears because of the non-flux boundary condition in the x-direction. Replacing these expansions in (1) it is found that

$$\langle \phi_{\mathbf{k}} \rangle = 0, \quad \langle \phi_{\mathbf{k}} \phi_{\mathbf{q}} \rangle = \gamma_{k_x} \hat{\delta}_{\mathbf{k},\mathbf{q}} V S^*(\mathbf{k}), \qquad (8)$$

with the same structure factor $S^*(\mathbf{k})$ as in the homogeneous case. Finally, the density field fluctuations in real space are given by:

$$\langle \phi(\mathbf{r}) \rangle = 0,$$
$$\langle \phi(\mathbf{r})^2 \rangle = \frac{\Gamma}{2 D k_0^2} V^{-1} {\sum_{\mathbf{q}}}' \frac{1}{q^2 + 1} \cos(q_x k_0 x)^2, \qquad (9)$$

where $\mathbf{q} = \mathbf{k}/k_0$ and the prime in the sum means that the term $q_x = 0$ has a factor 1/2.

The sum in Eq. (9) contains an ultraviolet divergence ($\mathbf{q} \to \infty$). Therefore, in order to perform the summation a regularization prescription is needed. The divergence is unphysical because it comes from assuming that the mesoscopic model (1) remains valid up to infinitely large wavevectors. Therefore, we introduce a regularizing kernel in Eq. (9) of the form $1/(1 + \epsilon^2 q^2)$, that equals 1 for $\epsilon \to 0$, limit that will be taken at the end of the calculations. The choice of a rational function instead of an exponential one is made to keep the calculations as simple as possible, but its form is immaterial. The technique of a regularizing kernel is equivalent to imposing a cutoff in the q-vectors of the order of $q_c \sim \epsilon^{-1}$ or to the *zeta* regularization [44].

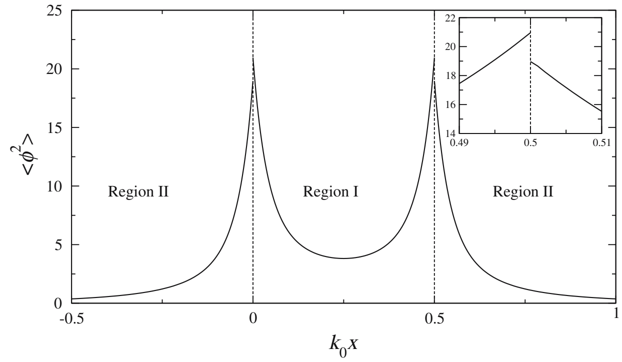

Fig. 1 Density fluctuations, calculated from Eq. (10) versus the scaled variable $k_0 x$. The cutoff value is $\epsilon = 0.01$, and the plates are at a scaled distance of $k_0 L = 0.5$. The vertical scale has arbitrary units and the asymptotic value of the density fluctuations, Eq. (13) has been subtracted. As seen, the density fluctuations between the plates (Region I) differs from the value outside the plates (Region II). The jump at the plates (that will produce the Casimir force) is shown in the inset

Next, we take the limit $L_y, L_z \to \infty$ allowing us to replace the sums on q_y and q_z by integrals that can be carried out, with the result:

$$\langle \phi(\mathbf{r})^2 \rangle = \frac{\Gamma}{8\pi D X} \frac{1}{1 - \epsilon^2} \times {\sum_{q_x}}' \log\left(\frac{1 + \epsilon^2 q_x^2}{\epsilon^2 (1 + q_x^2)} \right) \cos(q_x k_0 x)^2. \qquad (10)$$

The sets of q_x-vectors entering in this sum are different for Regions I and II, and therefore the density fluctuations. In Region I, the allowed q_x vectors are quantized as: $q_x = \pi n_x / (k_0 L)$, while in Region II they form a continuum in the limit $L_x \to \infty$. Figure 1 shows the density fluctuations (10) in the x-direction when the plates are located at $x = 0$ and $k_0 L = 1/2$, $\epsilon = 0.01$ and $L_x \to \infty$. The difference in q_x-vectors leads to a jump of $\langle \phi^2 \rangle$ at the plates, shown in the inset.

As shown in Fig. 1, the density fluctuations in a confined system depend on the position but also on the system size, and therefore are different in the region in between the plates and the region outside them. If the pressure is a function of the local density field $p(n)$, these differences in the density fluctuations create an unbalance of the pressure at both sides of each plate (see inset of Fig. 1), and consequently a net force. Note that when including the regularizing kernel into the sum (9) it turns out that a constant term in $S(\mathbf{k})$ leads to a size independent contribution to $\langle \phi^2 \rangle$ and therefore to the pressure. In consequence, the equilibrium part of the structure factor in Eq. (4) does not contribute to the Casimir forces, allowing to eliminate it form the calculations.

To calculate the force, we expand the local pressure around the reference density n_0, and take the statistical average, finding that

$$\langle p(x)\rangle \simeq p(n_0) + \frac{1}{2}\left.\frac{\partial^2 p}{\partial n^2}\right|_{n_0} \langle \phi(x)^2\rangle, \tag{11}$$

where higher order terms in the field have been neglected. The net force acting on the plate located at $x = L$ is the difference between the pressure inside $p(x \to L^-)$ and the pressure outside $p(x \to L^+)$. These values are calculated from Eq.(10), replacing the value of x by L (implying that $\cos(q_x k_0 L) = 1$) and using the appropriate set of q_x vectors. In the outer part of the plates, region II, the q_x vectors form a continuum and the sum is replaced by an integral:

$$\langle \phi^2\rangle_{II} = \frac{\Gamma}{8\pi DX}\frac{1}{1-\epsilon^2}\int dq_x \log\left(\frac{1+\epsilon^2 q_x^2}{\epsilon^2(1+q_x^2)}\right), \tag{12}$$

with the result:

$$\langle \phi^2\rangle_{II} = \frac{\Gamma}{4DX}\frac{1}{\epsilon(1+\epsilon)} \tag{13}$$

that diverges in the limit $\epsilon \to 0$ as $\mathcal{O}(\epsilon^{-1})$. The pressure in the inner region, written as

$$\langle \phi^2\rangle_{I} = \frac{\Gamma}{8\pi DX}\frac{1}{1-\epsilon^2}\sum_{q_x}{}' \log\left(\frac{1+\epsilon^2 q_x^2}{\epsilon^2(1+q_x^2)}\right), \tag{14}$$

with q_x forming a discrete set, $q_x = \pi n_x/(k_0 L)$, can be performed with the help of Eq. (1.431,2) of [45]. It also shows a divergence as $\mathcal{O}(\epsilon^{-1})$ with the same prefactor of Eq. (13). Therefore, in the net force between the plates by unit area, obtained as the pressure difference, both divergent contributions cancel. The result for the force is finite and in the limit of a vanishing cutoff ϵ, is simply

$$\begin{aligned} F/A &= \frac{1}{2}\frac{\partial^2 p}{\partial n^2}\lim_{\epsilon\to 0}\left[\langle\phi^2\rangle_I - \langle\phi^2\rangle_{II}\right], \\ &= F_0(1-\log(2\sinh l)/l), \end{aligned} \tag{15}$$

where $l = k_0 L_x$ and $F_0 = \Gamma k_0(\partial^2 p/\partial n^2)/(16\pi D)$. Let us note that the final expression of the Casimir force, is a *universal* function of the reduced distance, $l = k_0 L_x$. Moreover, there is no dependence on the cutoff length, as the two divergences in the cutoff, one stemming from the discrete sum and another from the integral, exactly cancel each other. The regularizing kernel, a technique well known in the field of Casimir forces [46], has allowed us to obtain a finite result as a difference of two diverging quantities.

The analysis of the Casimir force, Eq. (15) can be performed in the limits of far plates ($l \gg 1$) or near ones ($l \ll 1$). In the first case, ($l \gg 1$), implies that the distance $L_x \gg k_0^{-1}$ and therefore the plates are outside the correlation length, k_0^{-1} (see Eq. 4). Then, one expects a very fast decay of the Casimir forces. In the opposite limit ($l \ll 1$), when the plates are well inside the correlation length, the force is much stronger. The expression for these forces are

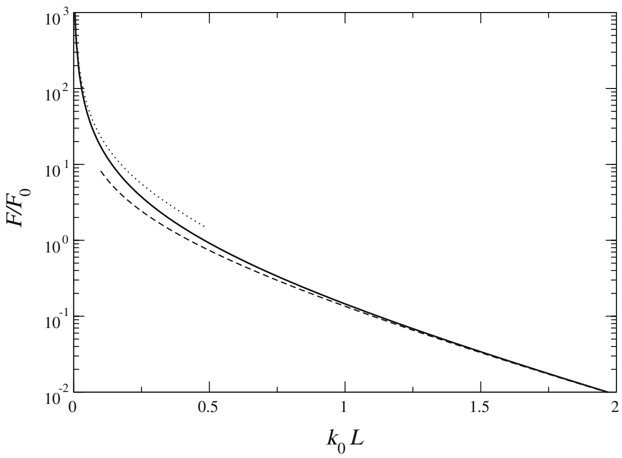

Fig. 2 Logarithm of the dimensionless force (Eq. 15) plotted as a solid line, versus the dimensionless distance $l = k_0 L$. Two different regimes are observed: for short distances, $l \gg 1$ (*dotted lines*) and long ones, $l \ll 1$ (*dashed line*)

$$F^{\text{far}}/A = F_0\frac{e^{-2l}}{l}, \quad F^{\text{near}}/A = -F_0\frac{\log l}{l}. \tag{16}$$

The expression of F^{near} is only valid for distances larger that any microscopic cutoff, otherwise the description based on continuum differential equations (1) becomes meaningless. Therefore no real divergence of the force is obtained for small distances.

In Fig. 2 we plot the exact force Eq. (15) as a function of the dimensionless distance l, together with the far and near plate approximations.

3 Casimir forces in granular fluids

In this section we will apply the concepts developed in Sect. 2 to a granular fluid in two dimensions. We will derive an effective Casimir force between two large immobile intruders immersed in a sea of small inelastic particles. This non vanishing force may explain some of the numerous segregation phenomena observed in granular mixtures [47–52]

We consider the driven granular model in [32,53]. Grains are hard particles of diameter d and mass m and their collisions are characterized by a constant normal restitution coefficient α. To achieve a stationary state, energy is supplied into the system by random forces acting on all particles. The random forces $\mathbf{F}_i$ are modeled as a white noise of intensity Γ: $\langle \mathbf{F}_i(t)\mathbf{F}_k(t')\rangle = m\Gamma\delta_{ik}\delta(t-t')$. The macroscopic equations that describe this inelastic fluid are the usual Navier Stokes fluid equations for the density (n), velocity ($\mathbf{u}$) and temperature (T) fields, supplemented with the terms that account for the energy dissipation plus the random forces. They read [32]:

$$
\begin{aligned}
&\partial_t n + \nabla \cdot (n\mathbf{u}) = 0\\
&\partial_t \mathbf{u} + \mathbf{u} \cdot \nabla \mathbf{u} = -\frac{1}{\rho} \nabla \cdot \mathbf{\Pi}\\
&\partial_t T + \mathbf{u} \cdot \nabla T = -\frac{2}{dn} (\nabla \cdot \mathbf{J} + \mathbf{\Pi} : \nabla \mathbf{u}) - \gamma + m^2 \Gamma^2,
\end{aligned}
\tag{17}
$$

where $\mathbf{J}$ is the heat flux and $\mathbf{\Pi}$ is the stress tensor. The quantity γ accounts for the collisional energy loss per unit time, given, in mean field approximation by: $\gamma = 2\gamma_0 \omega T$, being $\gamma_0 = (1-\alpha^2)/(4)$ and $\omega \propto \sqrt{T}$ the collision frequency. The term $m^2\Gamma^2$ is obtained averaging the kinetic energy per particle gained by the random collisions. These two contributions make the temperature a kinetic variable rather than a slow one. Still, it can be considered a slow variable for small inelasticities. Further analysis of the temperature equation shows that for a homogeneous system, the temperature reaches a stationary value determined by the balance of the last two terms: $\gamma = m^2\Gamma^2$. It can be shown that this stationary state is stable [32].

The set of hydrodynamic equations described above is not complete [32]. They miss the random terms coming from two sources:
(i) fluctuations of the random forces that inject energy at random times, and whose average value is given by Γ. Following the literature, we will call these terms *external*, and they contribute on the momentum and temperature equations. Their amplitudes are related with the intensity of the random forces and are of order $\mathcal{O}(k^0)$, where k is the wavevector, and therefore are the analogous to the term ξ_2 in Eq. (1).
(ii) internal fluctuations (Langevin type) coming from the discrete nature of the particles that form the granular fluid. The intensity of these Langevin fluctuations can be related with the transport coefficients of the fluid via an extension to non-equilibrium of the Fluctuation–Dissipation theorem. As usual in fluctuating hydrodynamics, they are of order $\mathcal{O}(k^2)$, like ξ_1 in Eq. (1) [25].

The homogeneous stationary state reached by this fluid is characterized by long range correlations between any two hydrodynamic fields A, B, of the form $G_{AB}(r) \propto 1/r$ in 3-dimensions and $G_{AB}(r) \propto -\ln(r)$ in 2-dimensions. In Fourier space the static structure factors are long ranged in all the k range. Their expression at small k are, after subtracting the $k \to \infty$ plateau: $S_{AB}(k) = S^0_{AB}/k^2$ where the coefficients S^0_{AB} depend on density, noise intensity and dissipation coefficient α. Explicit expressions for them can be found in [32]. These long range correlations lead to the renormalization of the energy density and collision frequency due to the fluctuations at low wave-vectors.

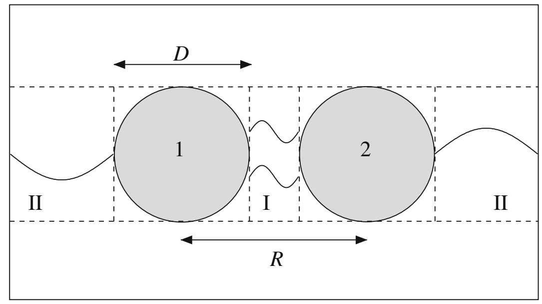

Fig. 3 Sketch of the configuration in the granular system. Two immobile intruders, 1 and 2, of diameter D are placed at a distance R. They are surrounded by fluid of small inelastic particles (not shown), whose fluctuations leads to the Casimir force. In the approximations of this paper, only fluctuations that fit in regions I or II are allowed. The allowed wave-numbers are $2\pi n/(R-D)$ and $2\pi n/(L-R-D)$, respectively

We consider now a system where, in addition to the small grains described as a granular fluid, two inelastic impenetrable and immobile large hard disks (the intruders) of diameter D are placed, separated at a distance R (see Fig. 3). The objective is to see if the confinement of the fluctuations, produced by these intruders, produce a Casimir force on them. The coefficient of restitution α is the same for all types of collisions. These two immobile disks play the role of the flat plates in Sect. 2, limiting the allowed wave-vectors of the hydrodynamic fields as will be discussed below.

To describe the Casimir force originated from the fluctuating hydrodynamic fields acting on the intruders we use an approach similar to Sect. 2, where the pressure is renormalized everywhere due to fluctuations that are computed using fluctuating hydrodynamics. In this case, the force over the intruders is produced by the pressure tensor, which is given at position $\mathbf{r}$:

$$
p^*(\mathbf{r}) = p(n(\mathbf{r}), T(\mathbf{r}))\; I + m\, n(\mathbf{r})\; \mathbf{u}(\mathbf{r})\; \mathbf{u}(\mathbf{r}), \tag{18}
$$

where n and T, and $\mathbf{u}$ are the instantaneous fluctuating density, temperature, and velocity fields and I the identity tensor, respectively. Moreover, the hydrostatic pressure $p(n, T) = T H(n)$ is the usual thermodynamic pressure for hard disks with $H(n) = n(1+\phi^2/8)/(1-\phi)^2$, and $\phi = \pi n d^2/4$ [54]. As the intruders are immobile, $\mathbf{u}$ vanishes at their surface, so the contribution of the convective term in p^* vanishes and it becomes a scalar. This would not be the case if the intruders were allowed to move.

In analogy with Eq. (11), we linearize the hydrodynamic fields $(n, T, \mathbf{u})$ around the stationary values, $(n_0, T_0, 0)$, and expand the pressure up to second order in the fluctuations δn and δT. Its statistical average over the random noise is

$$
\langle p^* \rangle = p_0 + H_1 \langle \delta T \delta n \rangle + T_0 H_2 \langle \delta n^2 \rangle, \tag{19}
$$

where $p_0 = p(n_0, T_0)$ and the coefficients H are derivatives of the pressure: $H_1 = dH/dn|_{n_0}$, $H_2 = \frac{1}{2} d^2H/dn^2|_{n_0}$. In

Fourier space the density-density and density-temperature fluctuations transforms into structure factors:

$$\langle p^* \rangle = p_0 + V^{-1} \sum_{\mathbf{k}} \left[H_1 \, S_{nT}(\mathbf{k}) + T_0 \, H_2 \, S_{nn}(\mathbf{k}) \right]. \tag{20}$$

The dominant contribution to the pressure comes from the region at small k, where they show a power law dependence $S_{AB}(\mathbf{k}) = S^0_{AB} \, k^{-2}$ described before. We then obtain:

$$\langle p^* \rangle = p_0 + V^{-1} \left[H_1 \, S^0_{nT} + T_0 \, H_2 \, S^0_{nn} \right] \sum_{\mathbf{k}} \frac{1}{k^2}. \tag{21}$$

Let us note that for the granular geometry there are not two *space-independent* regions, as it happened in the case studied in Sect. 2 where the infinite plates divided the space in three independent regions (or two if periodic boundary conditions were considered). Still the hydrodynamic fluctuations must vanish at the surface of the intruders, so that, in between the two intruders they have wave-vectors equal to $2\pi n/(R-D)$ being n an integer. Therefore as a first approximation we can suppose that the fluctuations in between the obstacles are restricted to have wave-vectors as in the region labeled I in Fig. 3, and outside them as in the region II. In detail, we perform the k-sum only over the k-vectors allowed by the geometrical constraints. In a rectangular box of size $a \times b$, the x-component of the k vectors is $2\pi n_x/a$ and the y component is $2\pi n_y/b$. It is at this point where the difference between regions I and II appears: $a = R - D$ in region I and $a = L - R - D$ in region II, while $b = D$ in both regions. By treating the regions as independent, we overestimate the pressure difference and hence the Casimir force, but obtain a first numerical approximation. Finally, this system owns a natural ultraviolet cutoff, given by $k_c = 2\pi/d_0$, where $d_0 = \max(d, l_0)$, and l_0 is the mean free path of the small particles. Beyond this cutoff the hydrodynamic description is no longer valid. It is equivalent to including a regularizing kernel with $\epsilon \simeq k_c^{-1}$.

The prefactor in the sum (21), $C \equiv H_1 \, S^0_{nT} + T_0 \, H_2 \, S^0_{nn}$ is dominated by the density–temperature fluctuations which are negative [55], as the collisional dissipation increases (so temperature decreases) with increasing density. The factor C turns positive for densities close to the close packing ($n > 0.73d^{-2}$), where the density–density fluctuations are more important. The fact that $C < 0$ implies that fluctuations produce a decrease of the local pressure. In the gap between the intruders (region I according to Fig. 3) the number of possible $\mathbf{k}$ modes of low k is smaller than outside (region II). The net effect is that the pressure is lower outside than inside, leading to an effective repulsive force between the intruders. Furthermore, C is proportional to the temperature, so is the Casimir force.

In the limit of small k, with structure factors going as k^{-2}, the pressure (20) can be analyzed asymptotically in the

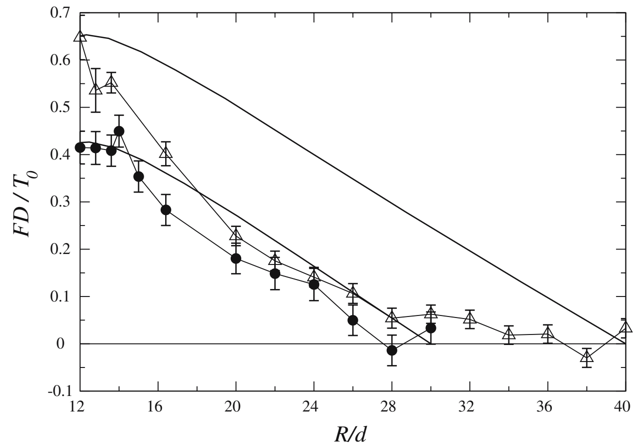

Fig. 4 Dimensionless Casimir force between the immobile intruders as a function of the distance R. Solid lines are the theoretical predictions derived in this paper, for two system sizes: $L = 80$ (*upper line*), and $L = 60$ (*lower line*). Simulation results are plotted as *open triangles* for $L = 80$ and *solid circles* for $L = 60$

cases $a \gg b$ (for particles at large distances) and $a \ll b$ (for particles at short distances)

$$\langle p^* \rangle = \begin{cases} p_0 + C\, a/b \; ; \; a \gg b \gg d_0 \\ p_0 + C\, b/a \; ; \; b \gg a \gg d_0. \end{cases} \tag{22}$$

Note that these asymptotic expressions for the renormalized pressure do not depend on the cutoff distance, as long as a and b are much larger than it. Finally, the effective force on the particle 2 is the difference of the forces at the left and the right of the particle $F_2 = D\left[\langle p^*_{\mathrm{I}} \rangle - \langle p^*_{\mathrm{II}} \rangle\right]$. A negative value of C gives rise to a long range linear repulsive force and a short range attractive force, at distances smaller than D. The opposite is obtained when C is positive. Note that in this estimate the force depends on the system size. This fact is related to the structure of the fluctuations, that become larger for small wave-vectors. Therefore, increasing the system size, while keeping R fixed, the fluctuations in region II become larger, decreasing even more the pressure in this region. However, as mentioned, at long distances this approximation is not completely valid.

The Casimir force is more accurately computed by using the full expression of the structure factors [32], rather than the k^{-2} part, valid for small k. The results are shown in Fig. 4 as solid lines plotted in dimensionless units. The intruders have a diameter $D = 8d$, the density equals $n = 0.366d^{-2}$ and dissipation is $\alpha = 0.8$. The force for two different systems sizes are plotted, for $L = 80d$ (upper line) and $L = 60d$ (lower line). This figure confirms the existence of a non-vanishing *long-range* force, extending for distances much larger than the particle diameters, d and D. The Casimir force shows a linear behavior in agreement with Eq. (22) (vanishing at $R = L/2$, due to periodic boundary conditions). At shorter distances, the force deviates from the linear expression (22), due to the corrections to the $1/k^2$ form of the structure factor.

In order to test the validity of the Casimir force obtained, we have performed numerical simulations of the granular system. Details of the computer simulations, specially how to implement the random collisions, are given in [56]. In the simulations we choose as basic units d, m, and Γ. These units define the time unit as $t_0 = (md^2/\Gamma)^{1/3}$ and energy unit as $e_0 = (md^2\Gamma^2)^{1/3}$. Given the density, restitution coefficient and noise intensity mentioned above, the stationary temperature can be computed using mean field models giving $T_0 = 1.84\, e_0$, and the collision frequency is $\nu_0 = 3.03\, t_0^{-1}$. This temperature T_0 is used to make the abscissa units non-dimensional. However, hydrodynamic fluctuations determine a stationary temperature higher than T_0 that depends on the system size [32]. For $L = 60\, d$, $T = 2.43\, e_0$ and for $L = 80\, d$, $T = 2.46\, e_0$. For every configuration, simulations were run for about 5×10^6 collisions per particle. In order to calculate the force, we measured the component of the total momentum transferred from the gas to intruders 1 and 2 along the line, parallel to the x-axis, joining their centers, P_{ix} ($i = 1, 2$) as an average over 100 collisions per particle. This procedure gives the "instantaneous" value of the fluctuating force as $F_{12} = \langle P_{2x} - P_{1x} \rangle / 2\tau$, whose time-average finally leads to the net effective force, F.

The simulated force is plotted in Fig. 4 for $L = 60d$ (solid circles) and $L = 80d$ (open triangles). As seen, there is qualitative agreement between theoretical and simulation results concerning the sign of the force and its magnitude, specially for intermediate distances. For large distances, however, our theory does not predict the saturation of the force observed for $R > 20d$. There are several possible sources for this discrepancy. The most important one is that hydrodynamic correlations between regions I and II are not independent. In fact, due to its long range nature, *any fluctuation* generated outside regions I and II will contribute to the pressure calculation in Eq. (21), reducing the pressure difference. Moreover, the presence of the fixed intruders breaks the Galilean invariance and may modify the structure factors at very short wavelengths, introducing a finite correlation distance equivalent to k_0 in the structure factors, that will look like Eq. (4). Finally, but probably less important, there are geometrical factors that arise from considering the regions I and II as rectangular instead of those bounded by circles.

The simulations also confirm the origin of the forces in long range correlations: in the elastic case, recovered when $\alpha = 1$ together with $\Gamma = 0$, the force vanishes. In this case long range correlations are absent, so only the term p_0 survives in (21). This term does not produce a force as it cancels at both sides of the particle. Moreover, we calculated the y component of the force for $\alpha < 1$, which was compatible with zero to numerical accuracy.

Non hydrodynamic scales, i.e. particle separation of order of d or smaller, are accessible for computer simulations. In this case, the force between the particles show an oscillatory behavior plotted in Fig. 5. This force, much stronger that the Casimir one, is equivalent to the depletion forces appearing in elastic fluids [57,58], which are explained by entropic arguments based on equilibrium statistical mechanics. Other recent works [59,60] confirm that depletion forces are present in granular mixtures.

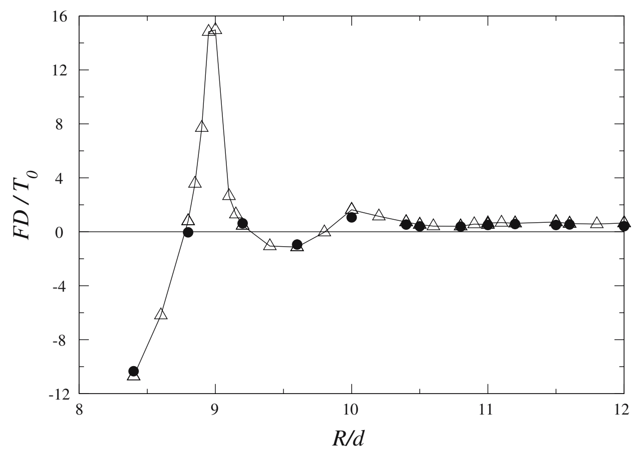

Fig. 5 Simulated force between the intruders for short distances, showing the typical oscillations of the depletion forces. Casimir theory, based in a continuum description of the fluid, cannot describe these short spatial scales

4 Conclusions

Casimir forces, as shown in this paper, are present for non-equilibrium systems, and can be calculated via the structure factors. The method presented here clarifies the role of the long range correlations, and their influence over the range of the force. Besides, in comparison with other methods that compute the size dependent stress tensor, this method is applicable to systems with no scale invariance (that is, with a finite correlation length). It has been illustrated for two physical systems and two geometries. The first one is a reaction-diffusion system described by a single scalar field whose correlation extend over a finite range characterized by k_0^{-1}. Two flat plates embedded in the system experience Casimir forces with the same range k_0^{-1} as the correlation length. For distances larger that k_0^{-1} the force decays exponentially.

A second application is to segregation in a binary granular fluid. The mixture is composed by two types of particles: one of them is much larger and heavier than the other, so they can be treated as immobile particles. In this case the correlations are long ranged with no characteristic decay length. Again, a non-vanishing Casimir force is obtained and their properties are analyzed, showing also to be long ranged.

The theory presented here show that three ingredients are needed in order to have a Casimir-fluctuating force:

(i) presence of long range correlations between the fluctuating fields,
(ii) confinement of fluctuations due to the presence of macroscopic objects (plates, spheres, etc),
(iii) an equation of state which is a nonlinear function of the fluctuating fields.

These ingredients are ubiquitous in non-equilibrium matter, in particular in granular materials.

Acknowledgments The authors want to thank C. Cattuto for performing the computer simulations in the granular case. R.B. is supported by the Projects MOSAICO, FIS2004-271 and UCM PR27/05-13923-BSCH. U.M.B.M. acknowledges a grant COFIN-MIUR 2005, 2005027808. R.S. is supported by Fondecyt research grants 1030993 and 1061112 and Fondap grant 11980002.

References

1. Casimir, H.B.G.: Proc. K. Ned. Akad. Wet. **51**, 793 (1948)
2. Lamoreaux, S.K.: Phys. Rev. Lett. **78**, 5 (1997)
3. Lamoreaux, S.K.: Phys. Rev. Lett. **81**, 5475 (1998)
4. Mohideen, U., Roy, A.: Phys. Rev. Lett. **81**, 4549 (1998)
5. Roy, A., Lin, C.-Y., Mohideen, U.: Phys. Rev. D **60**, 111101 (1999)
6. Milton, K.A.: J. Phys. A **37**, R209 (2004)
7. Kardar, M., Golestanian, R.: Rev. Mod. Phys. **71**, 1233 (1999)
8. Fisher, M., de Gennes, C.R.: C. R. Acad. Sci. Ser. B **287**, 207 (1978)
9. Stanley, H.G.: Introduction to Phase Transitions and Critical Phenomena. Oxford University Press, Oxford (1971)
10. Krech, M.: The Casimir Effect in Critical Systems. World Scientific, Singapore (1994)
11. Brankov, I., Danchev, D.M., Tonchev, N.S., Brankov, J.G.: Theory of Critical Phenomena in Finite-Size Systems: Scaling and Quantum Effects (Series in Modern Condensed Matter Physics, vol 9. World Scientific, Singapore (2000))
12. Forster, D.: Hydrodynamic Fluctuations, Broken Symmetry, and Correlation Functions. HarperCollins Canada, 1994
13. deGennes, P.G., Prost, J.: The Physics of Liquid Crystals. Oxford University Press, Oxford (1993)
14. Ajdari, A., Peliti, L., Prost, J.: Phys. Rev. Lett. **66**, 1481 (1991)
15. Ueno, T. et al.: Phys. Rev. Lett. **90**, 116102 (2003)
16. Martín, A. et al.: Phys. Rev. E **58**, 2151 (1998)
17. Cardy, J.L.: Conformal invariance. In: Domb, C., Lebowitz, J.L. (eds.) Phase Transitions and Critical Phenomena, vol 11. Academic, New York (1987)
18. Gambassi, A., Dietrich, S.: J. Stat. Phys. **123**, 929 (2006)
19. Dnatchev, D., Krech, M.: Phys. Rev. E **69**, 046119 (2004)
20. Dorfman, J.R., Kirkpatrick, T.R., Sengers, J.V.: Ann. Rev. Phys. Chem. **45**, 213 (1994)
21. Machta, J., Oppenheim, I., Procaccia, I.: Phys. Rev. Lett. **42**, 1368 (1979)
22. Lutsko, J.F., Dufty, J.W.: Phys. Rev. E **66**, 041206 (2002)
23. Procaccia, I., Ronis, D., Oppenheim, I.: Phys. Rev. Lett. **42**, 287 (1979)
24. Li, W.B. et al.: Phys. Rev. Lett. **81**, 5580 (1998)
25. Ortiz de Zárate, J.M., Sengers, J.V.: Hydrodynamic Fluctuations in Fluids and Fluid Mixtures. Elsevier, Amsterdam (2006)
26. Spohn, H.: J. Phys. A **16**, 4275 (1983)
27. Garrido, P.L. et al.: Phys. Rev. A **42**, 1954 (1990)
28. Grinstein, G., Lee, D.H., Sachdev, S.: Phys. Rev. Lett. **64**, 1927 (1990)
29. Pagonabarraga, I., Rubí, M.: Phys. Rev. E **49**, 267 (1994)
30. Gardiner, C.W.: Handbook of Stochastic Methods. Springer, Heidelberg (2004)
31. van Noije, T.P.C. et al.: Phys. Rev. Lett **79**, 411 (1997)
32. van Noije, T.P.C. et al.: Phys. Rev. E **59**, 4326 (1999)
33. Family, F., Vicsek, T. (eds.): Dynamics of Fractal Surfaces. World Scientific, Singapore (1991)
34. Kardar, M., Parisi, G., Zhang, Y.C.: Phys. Rev. Lett. **56**, 889 (1986)
35. Roters, L., Lübeck, S., Usadel, K.D.: Phys. Rev. E **59**, 2672 (1999)
36. Martınez, F.C. et al.: Phys. Rev. E **51**, 835 (1995)
37. Beijeren, H. van : J. Stat. Phys. **60**, 845 (1990)
38. Ernst, M.H., Bussemaker, H.J.: J. Stat. Phys. **81**, 515 (1995)
39. Suárez, A., Boon, J.P., Grosfils, P.: Phys. Rev. E **54**, 1208 (1996)
40. Baldassarri, A., Marini Bettolo Marconi, U., Puglisi, A.: Europhys. Lett. **58**, 14 (2002)
41. Ernst, M.H., Brito, R.: Phys. Rev. E **65**, 040301 (2002)
42. van Wijland, F., Oerding, K., Hilhorst, H.J.: Physica A **251**, 179 (1998)
43. García-Ojalvo, J., Sancho, J.M.: Noise in Spatially Extended Systems. Springer, New York (1999)
44. Ajdari, A. et al.: J. Phys. II France **2**, 487 (1992)
45. Gradshteyn, I.S., Ryzhik, I.M.: Table of Integrals, Series, and Products, 5th edn. Academic, New York (1994)
46. Bordag, M., Mohideen, U., Mostepanenko, V.M.: Phys. Reports **353**, 1 (2001)
47. Reis, P., Mullin, T.: Phys. Rev. Lett. **89**, 244301 (2002)
48. Aumaitre, S., Kruelle, C.A., Rehberg, I.: Phys. Rev. E **64**, 041305 (2001)
49. Schnautz, T. et al.: Phys. Rev. Lett. **95**, 028001 (2005)
50. Zuriguel, I. et al.: Phys. Rev. Lett. **95**, 258002 (2005)
51. Cattuto, C., Marini Bettolo Marconi, U.: Phys. Rev. Lett. **92**, 174502 (2004)
52. Kudrolli, A.: Rep. Prog. Phys. **67**, 209 (2004)
53. Peng, G., Ohta, T.: Phys. Rev. E **58**, 4737 (1998)
54. Verlet, L., Levesque, D.: Mol. Phys. **46**, 969 (1982)
55. van Noije, T.P.C., Ernst, M.H., Brito, R.: Phys. Rev. E **57**, 4891 (1998)
56. Cattuto, C. et al.: Phys. Rev. Lett. **96**, 178001 (2006)
57. Gotzelmann, B., Evans, R., Dietrich, S.: Phys. Rev. E **57**, 6785 (1998)
58. Crocker, J.C. et al.: Phys. Rev. Lett. **82**, 4352 (1999)
59. Sanders, D.A. et al.: Phys. Rev. Lett. **93**, 208002 (2004)
60. Bose, M. et al.: Phys. Rev. E **72**, 021305 (2005)